Proceedings of the 10th World Congress on Mechanical, Chemical, and Material Engineering (MCM'24)
Barcelona, Spain - August 22-24, 2024
Paper No. MMME 129
DOI: 10.11159/mmme24.129

Green Channel Effect of Cu Nanotwin Enhanced Silver Sintered Die Bonding to Produce SiC Power Modules with Low Porosity and High Strength

Tung-Han Chuang [1], Yen-Ting Chen[2]*, Devi Indrawati Syafei [3], Yin-Hsuan Chen[1,4], Seven Chang[5], and James Chen[5]

[1] Ag Materials Technology Co. (Amtc), Hsinchu Science Park, 30078 Hsinchu, Taiwan
[2] Institute of Materials Science and Engineering, National Taiwan University, 106 Taipei, Taiwan
[3] Taiwan Semiconductor Manufacturing Co. (tsmc), Hsinchu Science Park, 30078 Hsinchu, Taiwan
[4] Fraunhofer Institute for Reliability and Microintegration (IZM), 13355 Berlin, Germany
[5] PowerX Semiconductor Co. (POWERX), 302047 Hsinchu, Taiwan
*Address correspondence to E-mail: a5331812@gmail.com

Abstract – Silver sintered die bonding of SiC/Cr/nt-Cu chips with DBC ceramic substrates at 250 °C for 60 min with a pressure of 15 MPa achieved significantly reduction of porosity from 12.6 % to 4.4 % and increase of bonding strength from 24.3 MPa to 42.8 MPa under identical conditions in comparison to that of conventional SiC/Cr/coarse grained Cu metallized SiC chips. The sputtered nanotwinned Cu thin film possessed a high density (111) orientation of 91.2%, in contrast to a low proportion about 20% for the conventional coarse-grained Cu film. Interfacial cross-sectional analyses and fractography after shear tests reveal the beneficial effects of highly (111)-oriented nanotwinned Cu structure on Ag sintered die bonding, reducing delamination between interfaces compared to conventional Cu grain structures.

Keywords: Ag sintering, densely packed (111)-oriented, high diffusivity, nanotwinned copper, pressure assisted.

1. Introduction

Die bonding, also called die attachment, is an important process for the manufacturing of power modules, which plays a critical role for the reliability of products. Sintered silver pastes present a robust alternative to lead-containing die attach materials. Unlike solder die bonding method prone to intermetallic-related fatigue issues and has limit for the operation temperature of power devices [1], [2], sintered Ag pastes circumvent these concerns. These joints boast a melting point matching silver's at 961°C, enabling operations at elevated temperatures. For instance, as an exemplary substrate-attach material in power modules, sintered silver joints sustain operational temperatures of up to 200°C, impractical for Sn or Pb-based solders. Such elevated temperatures align with the requirements of wide-bandgap semiconductors like GaN and SiC, common in various operations [3]. Notably, the superior electrical and thermal conductivities of sintered silver compared to solders stand as critical advantages in various applications. However, the traditional silver sintered die bonding power module has a high porosity about 15 to 25%, and a typical bonding strength about 25 MPa.

Lu's group initially observed that a Cu film characterized by a high nanotwin density exhibited a tensile strength approximately ten times greater than conventional cg-Cu [4]. Notably, an nt-Cu film featuring a twin thickness of 15 nm, comprising grain sizes ranging between 100 nm and 1 µm with an average size of about 400 nm, demonstrated superior strength compared to both cg-Cu and ultrafine-grained Cu (ufg-Cu) [5]. Kim et al. (2010) conducted measurements of distinct GBs' individual resistance using four-probe scanning tunneling microscopy (STM) [6]. Their findings emphasized that the electron-scattering capacity of GBs relied significantly on the symmetry of grains. Specifically, the resistivity of Σ3 (TB) was calculated to be approximately 0.202×10^{-12} Ω/cm^2, significantly lower than that of other random boundaries, by one to two orders of magnitude. Moreover, Jing-Ye Juang et.al., 2018 was examined the Copper-to-copper direct bonding on highly (111)-oriented nanotwinned copper. It was found that the bonded nt-Cu has fewer voids at the bonding interface. In contrast, a region not bonded and numerous voids were found in the bonded polycrystalline Cu [7]. Showing highly (111)-oriented nanotwinned copper improved the diffusivity. Given the considerable interest in (111)-oriented and nanotwinned copper (nt-Cu) for its heightened surface diffusivity on the (111) plane, as discussed earlier, the accelerated surface diffusion facilitates low-temperature direct bonding within the temperature range of 150 to 200 °C, achievable under standard vacuum conditions ranging from 10^{-4} to 10^{-3} torr.

Liu et al. further proposed that the diffusion of Cu atoms across the surface of Cu films occurs in response to stress gradients, facilitating the filling of voids and gaps within the bonding interface [8]. Table 1 presents the surface diffusion coefficient on the (111) surface of Cu is 3 to 4 orders of magnitude faster than on other surfaces. Hence, the (111) surface diffusivity emerges as a pivotal factor influencing bonding duration and temperature. Research by Kotri et al. indicates that the diffusion barrier of Ag atoms on the (111) Cu surface within the Ag/Cu (111) system is lower compared to that in the Ag/Ag (111) system. This suggests a higher diffusion rate of Ag atoms on Cu (111) surfaces than on Ag/Ag (111) surfaces [9], [10]. Consequently, Ag atoms might dominate as the primary diffusing species, and the prevalent diffusion path may occur via grain boundaries due to the lower temperature conditions. Additionally, the interdiffusion of Cu and Ag might arise due to concentration gradients. This indicates the potential to lower bonding temperatures and high bonding strength for direct wafer bonding [8].

Table 1. Calculated Cu surface diffusivity on (111), (100), and (110) planes at various temperatures, ranging from 150 °C to 250 °C. Surface Diffusivity (cm^2/sec) [8].

$D_{Surf.}$\ Temp.	(111)	(100)	(110)
250 °C	1.22×10^{-5}	4.74×10^{-9}	3.56×10^{-10}
200 °C	9.42×10^{-6}	1.19×10^{-9}	5.98×10^{-11}
150 °C	6.85×10^{-6}	2.15×10^{-10}	6.61×10^{-12}

Although the above-mentioned direct bonding method through nanotwinned thin films is applicable for the wafer bonding or CoWoS bonding for 3D-IC packaging [11], it seems to be difficult for the die bonding of a chip to ceramic or PCB substrates due to the surface roughness of the substrates, inducing many voids or cracks at the interfaces. Increasing the bonding pressure might reduce the interfacial voids for Si die bonding, it is inadequate for the SiC chips owing to the brittle and weakness of the Si wafer, resulting breakage of the SiC chips under a limiting external pressure. Chuang et al proposed an innovative silver sintered die bonding technique through the employment of nanotwinned films to enhance the silver sintering reaction during the die bonding process, leading to the benefits of low porosity and high strength for power modules [12], [13]. The present paper discloses an additional embodiment for the manufacturing of SiC power modules with backside metallization of Cr adhesive thin film and Cu reaction layer. The principle of this method utilized a nanotwinned Cu layer with a high density (111) preferential orientation to attain the advantage of high atomic diffusivity to promote the silver sintered die bonding process. Such high diffusive (111) nanotwins, acting as a “Green channel” (quick transportation path for sintering Ag atoms) to effectively reduce the porosity and increase the bonding strength of due bonding power modules.

2. Experimental

The die bonding experimental is conducted by using hybrid Ag paste from NAMICS coorperation company. With high-thermal-conductivity adhesives that meet RoHs requirements. NAMICS’ H9890 series, a low-temperature sintering silver paste seamlessly integrated with resin reinforcement and cutting-edge low-modulus technology. With thermal conductivity of 60 W/mK, a modulus of 6.5 GPa, and die shear strength of 50 N/mm². The substrate employed in this study comprised a direct bonding copper (DBC) alumina substrate with dimensions of 7 × 5 mm². The backside of the DBC substrate featured electroless nickel/immersion gold (ENIG) surface treatment, consisting of a Ni(P) layer measuring 4.5 μm in thickness, followed by a 100 nm Au layer. The die chips, composed of SiC/Cr/nt-Cu and SiC/Cr/Cu. The sintered die bonding process was conducted in a vacuum hot pressed furnace of 5x10-3 Torr with a temperature profile: Initially, dwell temperatures (TD) of 100°C were sustained for 60 minutes, followed by exposure to sintering temperatures (TS) set at 150°C, 200°C, and 250°C, for an additional 60 minutes, under an applied pressure of 15 MPa.

For the metallization process, n-type 4H-SiC wafers with dimensions of 4 inches in diameter and a thickness ranging from 350 ± 25 μm were employed. The resistivity of these wafers varied within the range of 0.015 to 0.028 Ω·cm. Subsequently, the wafers were sectioned into pieces measuring 4 mm × 4 mm. Preliminary cleaning was executed using acetone and alcohol to eliminate visible contaminants. The deposition of the target material onto the silicon carbide substrate to create thin films was carried out using a magnetron sputtering system (JUNSUN TECH, SGS500). The method to create high density (111) textured nanotwinned Cu thin films on SiC wafers has been reported by Chuang et al. [14], [15]. To optimize film quality, all depositions were conducted at a chamber pressure of 5 × 10−6 torr (6 × 10−4 Pa) and an argon (Ar) working pressure of 5 × 10−3 torr (0.67 Pa), employing a power of 300 W.

The Focused Ion Beam (FIB) procedure involved the utilization of a Hitachi NX2000 system with gallium (Ga) as the ion source. This process facilitated the transformation of liquid gallium into a Ga ion beam through the influence of

an external electric field. Conducting detailed structural analysis, a field-emission scanning electron microscope (Jeol JSM-7800F Prime) was deployed, integrating Electron Backscatter Diffraction (EBSD) to collect information on crystal structures, grain orientations, and related data. This method also provided imaging through secondary electron and backscattered electron modes. The determination of crystal orientations in surface films was accomplished through X-ray diffraction analysis (XRD Rigaku TTRAX), allowing for comparisons with EBSD results. Furthermore, a scanning Electron Microscope (SEM) cross-sectional analysis was employed to scrutinize the microstructure of sintered silver layers. Samples were encapsulated in epoxy resin, bisected along the sample center, and subjected to mechanical grinding and polishing of the cross-section to ensure the integrity of chip connections. The assessment of adhesion and die-bonding strength of thin films was conducted through a die shear test in accordance with MIL-STD-883 testing standards. The test utilized a DAGE4000 bond tester equipped with a 100 kg Die Shear (DS100) cartridge, capable of measuring a maximum push force of 100 kg.

3. Results and Discussion

Focused ion beam (FIB) metallography images in Fig. 1 show the cross-section of conventional backside metallization of equiaxed coarse grained copper films sputtered onto silicon carbide (SiC) substrates previously coated with a 100 nm chromium (Cr) layer. Fig. 1 reveals that such a copper film exhibited a polycrystalline structure characterized by disorderly equiaxial coarse grains with an absence of discernible twin formations. The discernment of a perpendicular growth pattern of coarse grains relative to the SiC substrate implies a preferential directionality in the epitaxial association between the copper film and the crystalline SiC substrate. The crystal lattice of the substrate functions as a directive template, dictating the alignment of developing grains in a direction perpendicular to its surface.

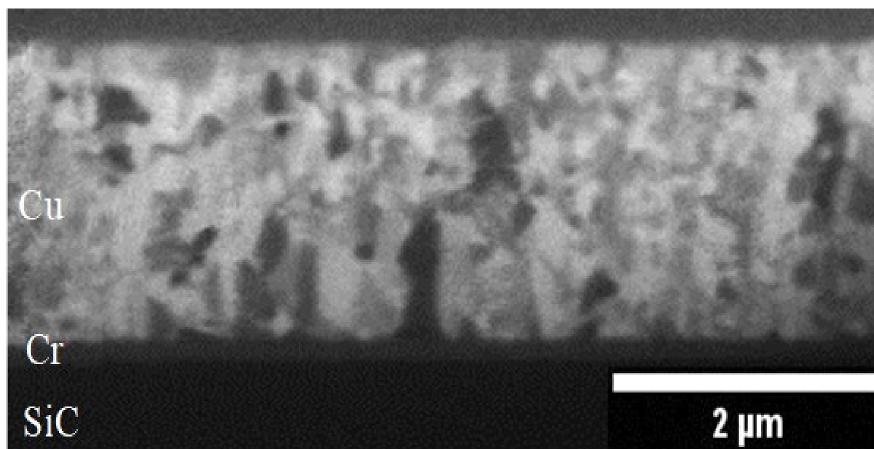

Fig. 1. FIB metallography of the cross-section of equiaxial coarse grained Copper with Cr adhesive layer on SiC substrate.

In comparation with the conventional backside metallized equiaxial coarse grained copper, Fig. 2 shows the nanotwinned copper (nt-Cu) reaction layer on Cr adhesive SiC chips that exhibited two distinct layers delineated by dashed lines, marking the boundary known as the transition layer. Beneath this transition layer, the film comprised disordered grains. Above this boundary, the film displayed a distinct layer characterized by nanotwinned columnar grains, exhibiting a unique and well-defined arrangement. These columnar copper grains were notable for the abundance of nanotwins present within them, contributing significantly to their distinctive structural characteristics. The nanotwinned copper (nt-Cu) layer exhibited a thickness of approximately 4 µm, contributing substantially to the film's overall composition. Additionally, the structure included a chromium (Cr) layer with an approximate thickness of 100 nm, serving as another integral component of the overall film architecture. Compared to the previously sputtered copper nanotwinned structures, the current vapor deposition process yields a more orderly copper film in columnar grain structure, with a less pronounced transition layer. There are lesser randomly oriented grains within the upper layer of nanotwinned structure, indicating a superior quality of nanotwinned structure in the vapor-deposited film.

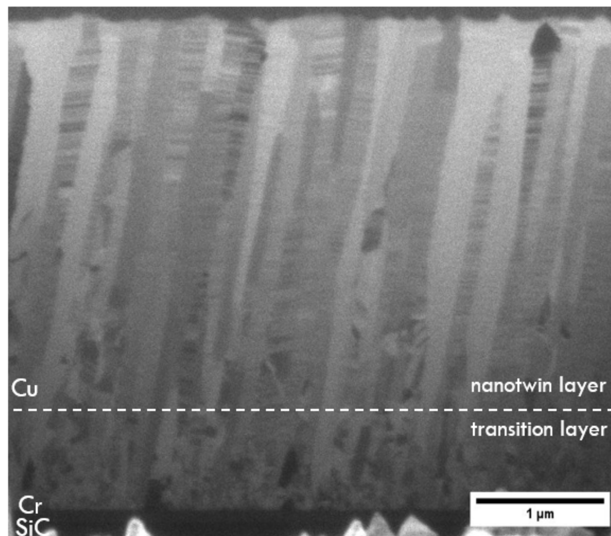

Fig. 2 Cross-sectional FIB metallography of nanotwinned Copper with Cr adhesive layer on SiC substrate

Substrate bias significantly influences the generation and growth of nanotwin structures, resulting in alterations in microstructures and crystallographic orientations, as evidenced by previous findings [16], [17], [18]. In the context of copper, an FCC metal, the (111) plane stands as the most densely packed, enabling an exceptionally rapid diffusion path, approximately three to four orders of magnitude faster than other planes such as (100) or (110) [19], [20]. The EBSD inverse pole figure (IPF) scan image in Fig.3a illustrates the top view of the copper film without negative substrate applied, revealing the normal direction (ND) of the grains. The blue-colored grains signify a crystallographic orientation along the <111> direction, indicating a substantial <111> preferred orientation. Employing OIM analysis software allowed determination of the locations and proportions of coincident boundaries. Quantification of the proportion of general grain boundaries and CSL-Σ3 twin boundaries was achieved through the distribution of misorientation angles. It resulted in a grain structure of 5% Coincidence Site Lattice (CSL-Σ3) boundaries and 2.4% CSL-Σ9 boundaries concerning the total grain boundaries, constituting very low proportion. The Focused Ion Beam (FIB) cross-sectional ion images demonstrated that the copper film displayed a polycrystalline structure (Fig.1) in the absence of substrate bias. In Fig. 3a, the surface EBSD map revealed an irregular grain orientation without a prominent preferred orientation, characterized by a mere 20% (111) proportion which correlates with the results of a low proportion of (111)-oriented grains.

The provided Fig. 3b present plane view electron backscatter diffraction (EBSD) inverse pole figure (IPF) images of the evaporated SiC/Cr/nt-Cu structure. Upon analyzing the EBSD inverse pole Fig. mapping, it was determined that the proportion of coincident site lattice (CSL) Σ3 boundaries to the overall grain boundaries amounts to 44.2%, while Σ9 boundaries constitute a smaller fraction, accounting for only 1.1% of the total measured grain boundaries. Subsequent observations using EBSD to analyze the surface crystallographic orientation in nanotwinned copper films, Fig. 4b revealed that the film surfaces exhibited (111) grains. The calculation results from the OIM software showed that the proportion of (111) grains on the film surface could reach a high density of 91.2%.

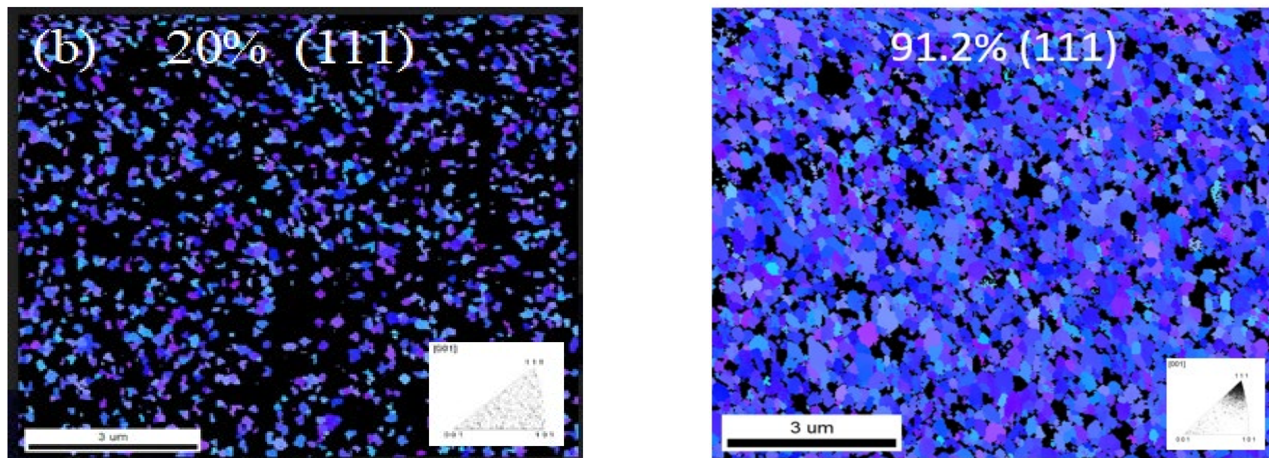

Fig. 3. Top-view EBSD inverse pole figure (IPF) maps showing (111)-orientation for: (a) SiC/Cr/coarse grained Cu film and (b) SiC/Cr/nt-Cu film.

The sintering process, crucially dependent on required relatively high temperatures and pressure as per previous investigations [21], exhibits notable microstructure evolution, as depicted in Fig. 4. At an initial temperature of 150°C, silver particles agglomerate with neighboring particles, possibly occurring before sintering. These agglomerated blocks display a distinct boundary, the inside of these blocks was not completely sintered, although with remaining gaps between the particles, albeit smaller than before. This initial agglomeration reduces the high surface energy of the nanoparticles. Subsequently, as the sintering progresses at higher temperatures (200°C), small sintered necks form between the particles within the agglomeration due to surface diffusion and grain boundary diffusion. At 250°C, observable densification takes place: the gaps between particles diminish, sintering necks expand, grains merge, and voids gradually disappear. Fig. 4 illustrates the significant reduction of gaps within the agglomerates, highlighting the evolution of the sintering process. Affected by concentration gradients and dominated by volume diffusion and gas phase transport, voids within the agglomeration gradually diffuse outward. The pivotal parameters of temperature and pressure significantly influence the sintering process [21]. Elevated temperatures enhance the mobility of surface atoms, while applied pressure facilitates intimate contact between surfaces and hybrid Ag particles, ensuring a robust adhesive connection. During such a pressure-assisted Cu annotwin assisted Ag sintering process, nanosilver particles experience tighter compression, leading to a larger contact surface area compared to pressureless sintered particles. This results in the formation of a greater number of sintering necks with larger contact areas, thereby enhancing the bonding quality and overall performance of the sintered layer.

The gradual densification of the sintered microstructure alongside decreasing porosity as sintering temperature increases indicates significant mass transfer between Ag particles. This process is instrumental in altering the surface morphology of the Ag paste [22]. It is noteworthy that the presence of pores can diminish mechanical, thermal, and electrical properties [23]. Moreover, the augmentation of raising sintering temperature accompanying with external pressure contributes to increased density by inducing deformation in Ag particles, enlarging the contact area among particles. The intensified sintering pressure aids solid diffusion at the interfaces, thereby enhancing bonding quality[24]. Fig. 5 shows the porosity reduction and bonding strength increase of Cu nanotwinned sintered die bonding specimens as a function of sintering temperatures with applied pressure of 15 MPa.

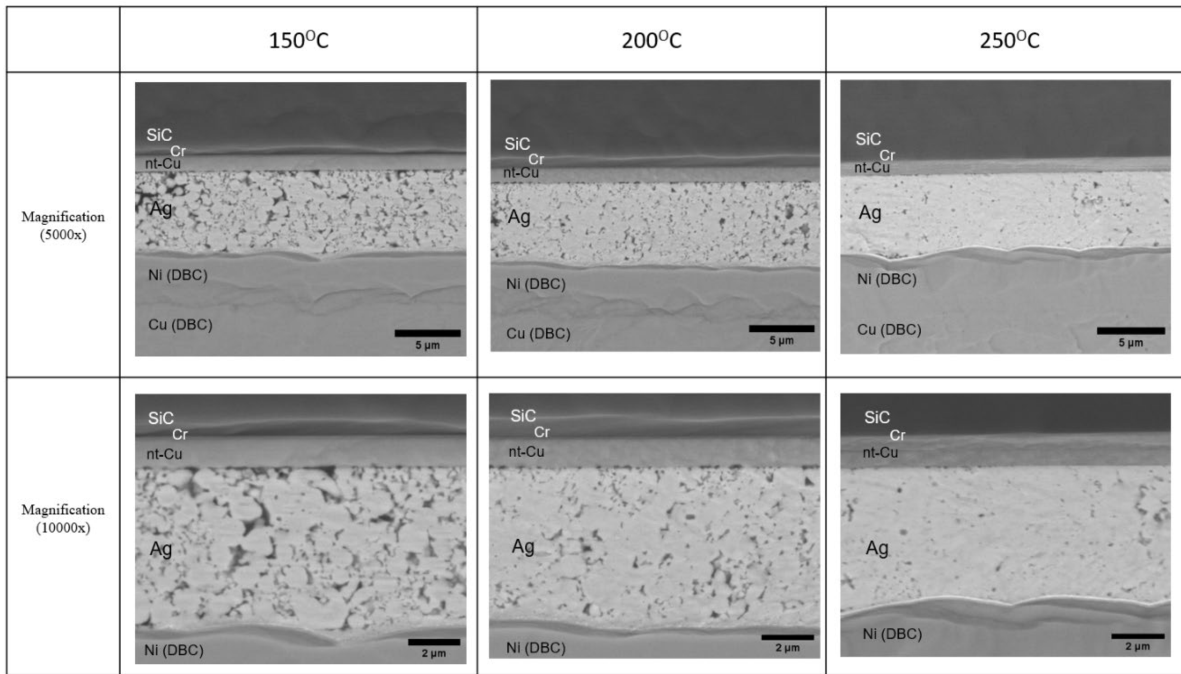

Fig. 4. The cross-sectional microstructure evaluation of Ag sintered die bonding of Cr/Cu nanotwinned metallized SiC chips with DBC substrates at various sintering temperatures: 150oC, 200oC, and 250oC, pressure-assisted 15 MPa.

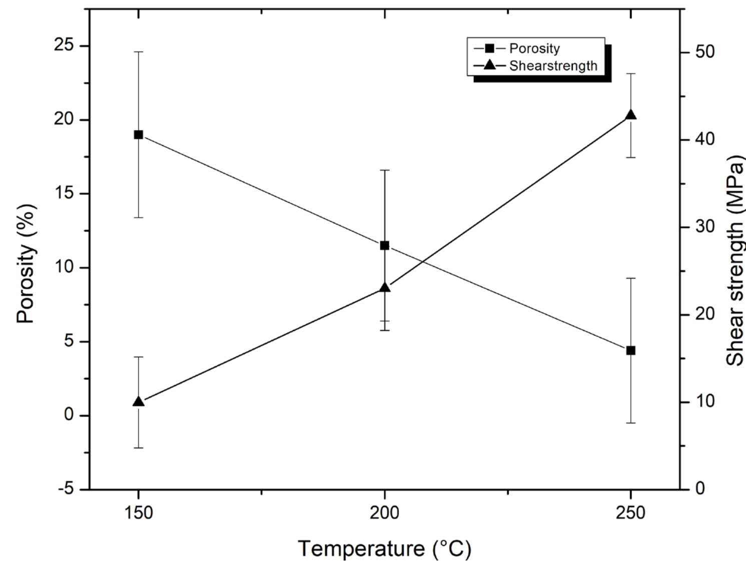

Fig. 5. Relation between porosity and shear strength of Ag sintered die bonding of Cr/Cu nanotwinned metallized SiC chips with DBC substrates under different temperature with pressure 15 MPa.

In the context of Ag sintered die bonding of Cr/Cu metallized SiC chips with DBC alumina substrates, the influence of high density (111) textured from nanotwinned Cu films manifests significantly. Comparing Ag sintering between conventional coarse grain Cr/Cu non-nanotwinned metallized SiC chips and those featuring nanotwinned Cu films revealed noteworthy differences, as depicted in Fig. 6. The fracture morphology of the sintered Ag, observed in the magnified micrograph of Fig. 6, demonstrates a ductile failure mode characterized by a dimpled structure. Ductile fracture surfaces typically display a dull, fibrous appearance, with dimples resembling weaver birds' nests when viewed perpendicularly. These dimples result from the initiation and coalescence of micro-voids around particles, expanding with continued deformation, eventually leading to the separation of material ligaments. The scooped-out regions within

these dimples often contain undissolved or precipitated particles, indicating the origins of void formation. In the case of Ag sintered with coarse grain Cr/Cu non-nanotwinned on DBC substrate, higher porosity is evident, leading to delamination between the Cu and Ag sintered layers. The presence of regions indicated by EDS spectrums as Cu, not covered by sintered Ag particles on the die chip side, illustrates the interfacial failure mode primarily due to lattice mismatch between Cu and Ag. This is characterized by extensive delamination and higher porosity at the Cu die - sintered Ag interface, as shown in Fig. 7 through cross-sectional FIB morphology. In contrast, the fracture morphology of Ag sintered die bonding of Cr/Cu nanotwinned metallized SiC chips with DBC substrates demonstrates better interface bonding between nt-Cu die chip and sintered Ag as shown in Fig. 8. The presence of fractures on the DBC substrate provides evidence that the highly (111)-oriented Cu nanotwinned structure significantly influences Ag sintering, enhancing surface diffusivity and atomic diffusion at film interfaces [25].

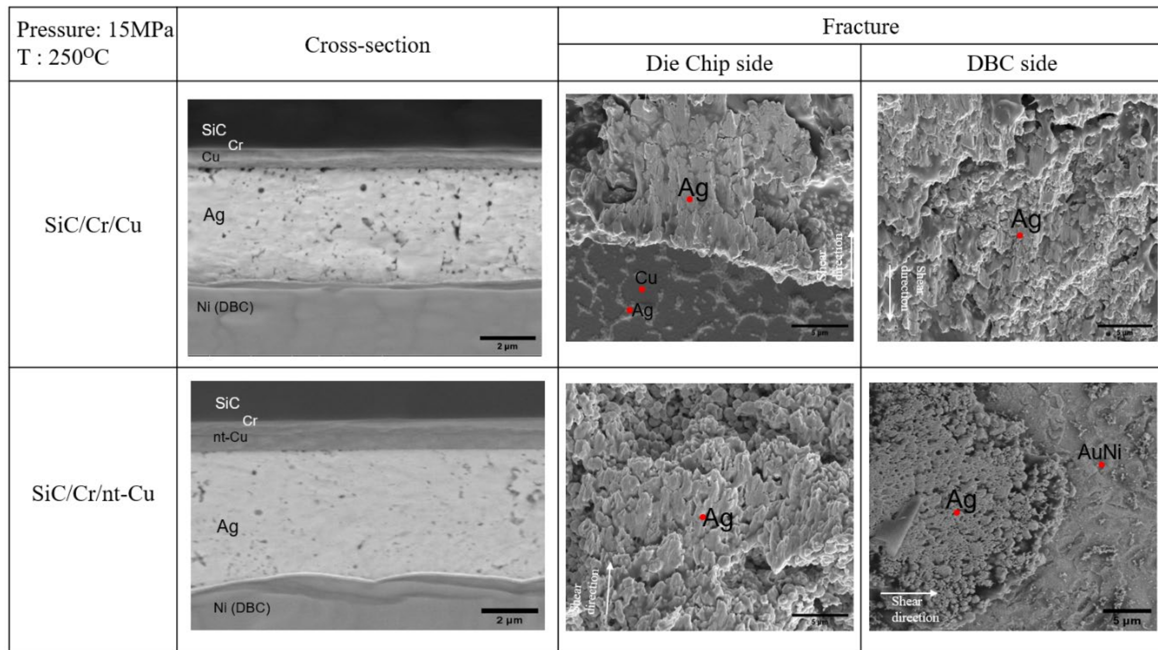

Fig. 6. The cross-sectional and fracture microstructure evaluation of Ag sintered die bonding of Cr/Cu grain and Cr/Cu nanotwinned metallized SiC chips with DBC substrates at 250oC, with pressure-assisted 15 MPa.

SEM microstructure cross-sections unveiled a threefold increase in porosity in the Ag-sintered coarse grain Cr/Cu non-nanotwinned chips in contrast to the high-density (111)-oriented nanotwinned Cu configurations. Table 2 elucidates the comparative porosity and shear strength outcomes of the two metallized chip configurations, SiC/Cr/Cu, and SiC/Cr/nt-Cu, when bonded to DBC substrates. The data are plotted in Fig. 7. Impressively, the porosity of Ag sintered SiC/Cr/nt-Cu chips with DBC ceramic substrates decreased from 12.6 % to 4.4 %, leading to a substantially higher shear strength of 42.8 MPa, marking a 24.3 MPa difference compared to the SiC/Cr/Cu chips sintered under identical conditions. These results underscore the advantageous impact of high-density (111) textured from nanotwinned Cu films on silver sintered die bonding. The presence of nanotwinned Cu films with highly density of (111)-orientation augments atomic diffusion across twin boundaries, enhancing interdiffusion between layers and ultimately yielding a stronger joint, reduced porosity, and heightened mechanical strength. The coherent crystal structure across twin boundaries plays a pivotal role in uniformly transmitting stress, fortifying the material's overall mechanical integrity. These findings underscore obviously the beneficial effects of high-density (111) textured Cu nanotwinned films on the silver sintered die bonding process.

Table 2. Porosity and shear strength of Ag sintered die bonding of Cr/coarse-grained Cu and Cr/nanotwinned Cu metallized SiC chips with DBC alumina substrates at 250oC for 60 min under 15 MPa pressure.

Temperature (°C)	**Porosity (%)**		**Average of Shear strength (MPa)**	
	SiC/Cr/Cu	SiC/Cr/nt-Cu	SiC/Cr/Cu	SiC/Cr/nt-Cu
250	12.6	4.4	24.3±6.3	42.8±4.8

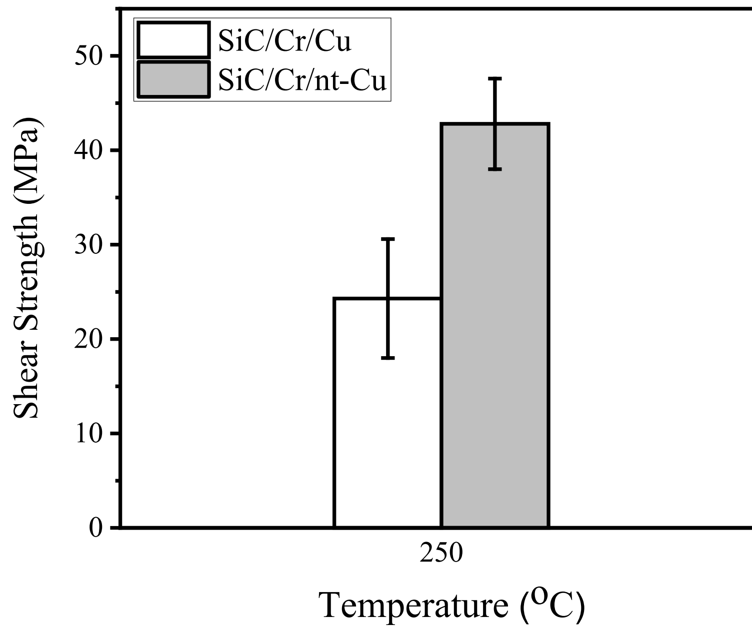

Fig. 7. Comparison of the shear strengths of Ag sintered die bonding of Cr/coarse grained Cu and Cr/nanotwinned Cu metallized SiC chips with DBC substrates at 250oC with external pressure 15 MPa.

The appearance of large voids in SiC chips backside metallized with conventional Cr/ equiaxed coarse grained Cu film after Ag sintered die bonding can further be conformed in Fig. 8. In the case of face-centered cubic (FCC) metals like copper (Cu), the (111) crystal orientation exposes densely packed atomic planes with high symmetry. The atomic arrangement in the (111) plane allows for tight packing of atoms, resulting in a stable and lower-energy surface configuration compared to other crystal planes. Consequently, Cu (111) crystal orientations tend to exhibit enhanced adhesion and stronger bonding behavior compared to conventional Cu coarse grain non-nanotwinned particles. Moreover, as illustrated in Fig. 9, the cross-sectional FIB micrograph shows the highly (111)-oriented Cu nanotwinned structure significantly influencing Ag sintering. This orientation facilitates surface diffusivity enhancement and atomic diffusion at film interfaces, presenting lesser delamination between interfaces compared to Fig. 8. Additionally, the nano-twinned columnar grains remain after the sintering process. This enhanced atomic diffusion, in conjunction with reduced surface energy barriers, enables successful bonding at relatively low temperatures. The lower surface energy and optimized atomic arrangement in the (111) plane promote stronger interfacial interactions with Ag sintered particles, resulting in improved adhesion between the Cu layer and the Ag particles. This improved adhesion significantly contributes to enhanced bond strength. Further, the optimized atomic arrangement in Cu (111) crystal orientations nanotwin facilitates more intimate contact and stronger chemical interactions with Ag sintered particles, establishing a more stable interface. This stability prevents delamination or separation between the Cu layer and the Ag particles, thereby augmenting the overall integrity of the bond.

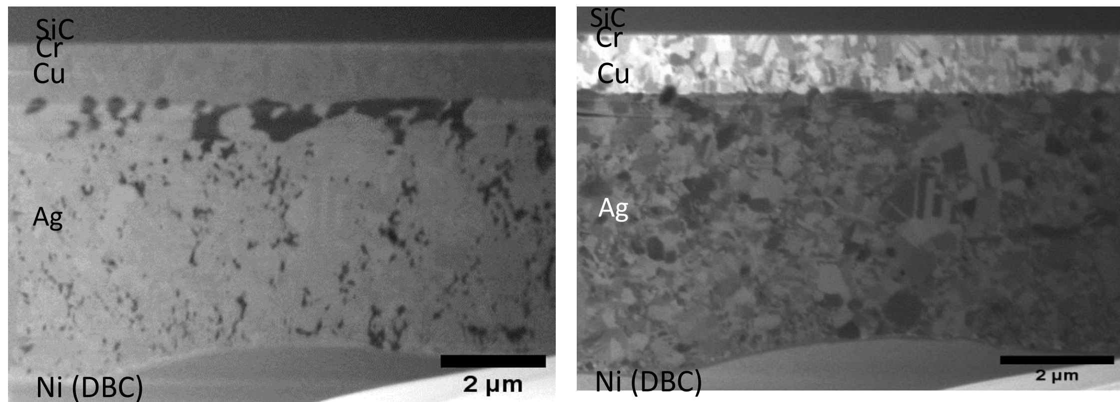

Fig. 8. The appearance of Cross-sectional FIB (a) electron image and (b) ion image of Ag sintered die bonding of Cr/Cu grain metallized SiC chips with DBC substrates at 250oC, with external pressure 15 MPa.

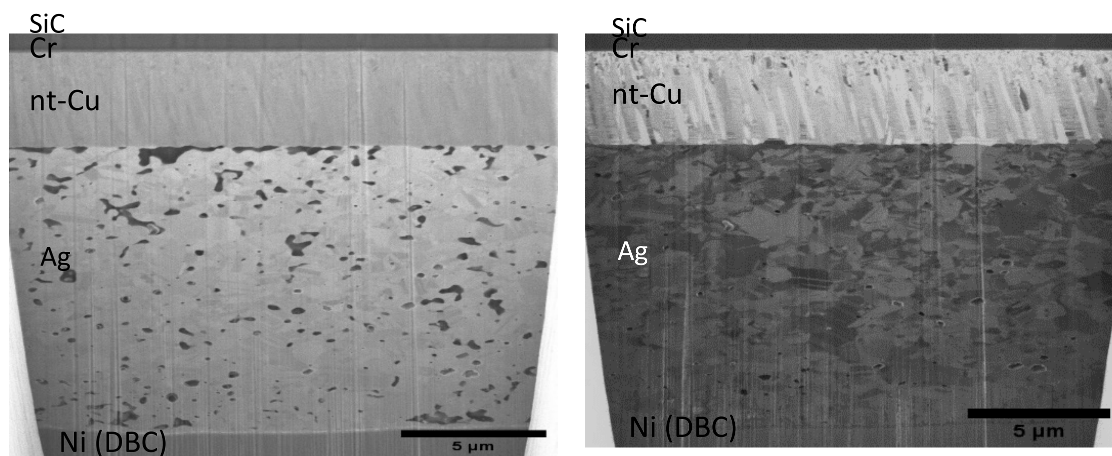

Fig. 9. Cross-sectional FIB (a) electron image and (b) ion image of Ag sintered die bonding of Cr/Cu nanotwinned metallized SiC chips with DBC substrates at 250oC, with external pressure 15 MPa.

The principle of porosity reducing and strength increase for the nanotwinned film enhanced Ag sintered die bonding was declared with a "Green channel" model proposed by Chuang et al [26] as demonstrated in Fig.10. It is known that twin boundaries within the crystal structure of nanotwins represent distinct interfaces, where atomic planes on one side mirror those on the other side. Such a lattice arrangement creates a highly ordered structure and acts as pathways for atoms to move across layers, from the nanotwinned Cu layer to the Ag paste layer, enhancing the quality of interfacial bonding. Fig. 10 illustrates their organized structure, providing a defined route for atomic transporation compared to regions lacking such organized interfaces. Overcoming energy barriers associated with atomic arrangement and bonding is crucial for atom movement. Twin boundaries lower these energy barriers, creating a more favorable environment for atomic migration [27]. The structured arrangement of highly (111)-oriented nanotwins Cu reduces the energy needed for atoms to traverse interfaces [25]. This reduction in activation energy facilitates more energetically favorable atomic diffusion along these paths, accelerating atomic migration compared to areas without organized interfaces. Structured twin boundaries significantly assist in atomic diffusion by offering pathways with lower resistance to atomic movement, enabling faster atomic diffusion across the interfaces between the (111)-oriented nanotwin Cu and Ag paste layers. The facilitated Ag atomic diffusion along the twin boundaries strengthens the overall integrity of die bonding. and toughness. The decrease of porosity and enhancement of bonding strength create a more durable and reliable power modules.

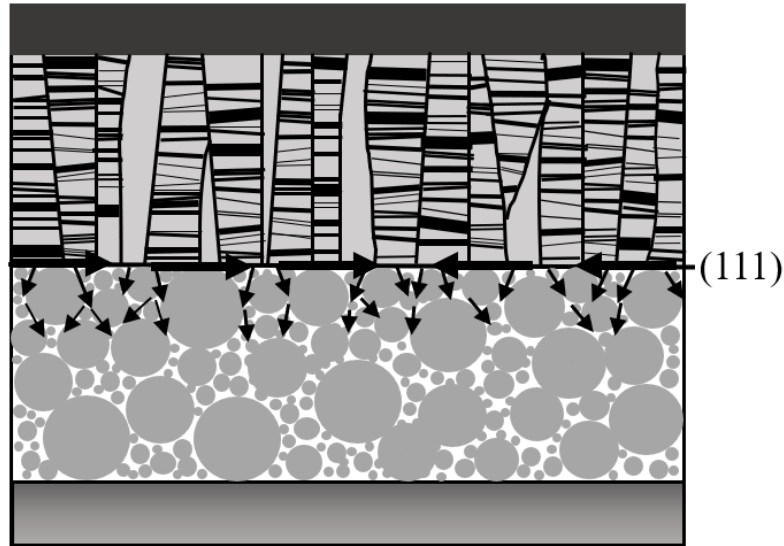

Fig. 10. Illustration for the “Green channel” effect of high density (111) orientation nanotwinned film on the densification of Ag sintered particles [12].

4. Conclusions

In summarizing, this study delves into potential improvements achievable through the utilization of (111)-textured Cu nanotwinned films compared to conventional backside metallization of equiaxed coarse grained Cu for silver sintered die bonding process. The assessment of porosity and bonding strength, underscores the importance of understanding how variations in sintering conditions influence the performance of die bonding power packages. Results from the study reveal that the Cu nanotwins significantly reduce the porosity of the sintered layer from 12.6% to 4.4% at 250°C for 60 min under 15 MPa pressure, contributing to improved mechanical properties. The highest shear strength, reaching 42.8 MPa at 250°C with pressure assistance in Ag sintered die bonding of Cr/Cu nanotwinned metallized SiC chips with DBC substrates, surpasses SiC/Cr/Cu chips sintered under identical conditions by 24.3 MPa. The cross-sectional FIB micrograph further illustrates the impact of the highly (111)-oriented Cu nanotwinned structure on Ag sintering, highlighting its role in reducing delamination between interfaces compared to conventional Cu grain structures. This observation emphasizes the advantages of high diffusivity through the (111) oriented nanotwinned Cu film for the die bonding of SiC chips with DBC substrates. This comprehensive exploration of “Green channel” effect for nanotwin enhanced silver sintered die bonding technique underscores the potential benefits in power modules manufacturing.

Acknowledgements

This study was sponsored by the industrial and academic cooperation program of National Taiwan University, 106 Taipei, Ag Materials Technology Co., (Amtc), Hsinchu Science Park, 30078 Hsinchu, and PowerX Semiconductor Co. (POWERX), 302047 Hsinchu, Taiwan.

References

[1] K. S. Siow and Y. T. Lin, ‘Identifying the development state of sintered silver (Ag) as a bonding material in the microelectronic packaging via a patent landscape study’, *J Electron Packag*, vol. 138, no. 2, p. 020804, 2016.

[2] H. L. J. Pang, K. H. Tan, X. Q. Shi, and Z. P. Wang, ‘Microstructure and intermetallic growth effects on shear and fatigue strength of solder joints subjected to thermal cycling aging’, *Materials Science and Engineering: A*, vol. 307, no. 1–2, pp. 42–50, 2001.

[3] Buttay, C., Planson, D., Allard, B., Bergogne, D., Bevilacqua, P., Joubert, C., ... & Raynaud, C.., ‘State of the art of high temperature power electronics’, *Materials Science and Engineering: B*, vol. 176, no. 4, pp. 283–288, 2011.

[4] L. Lu, Y. Shen, X. Chen, L. Qian, and K. Lu, ‘Ultrahigh strength and high electrical conductivity in copper’, *Science (1979)*, vol. 304, no. 5669, pp. 422–426, 2004.

[5] L. Lu, X. Chen, X. Huang, and K. Lu, ‘Revealing the maximum strength in nanotwinned copper’, *Science (1979)*, vol. 323, no. 5914, pp. 607–610, 2009.

[6] Kim, T. H., Zhang, X. G., Nicholson, D. M., Evans, B. M., Kulkarni, N. S., Radhakrishnan, B., ... & Li, A. P., 'Large discrete resistance jump at grain boundary in copper nanowire', *Nano Lett*, vol. 10, no. 8, pp. 3096–3100, 2010.
[7] Juang, J. Y., Lu, C. L., Chen, K. J., Chen, C. C. A., Hsu, P. N., Chen, C., & Tu, K. N., 'Copper-to-copper direct bonding on highly (111)-oriented nanotwinned copper in no-vacuum ambient', *Sci Rep*, vol. 8, no. 1, p. 13910, 2018.
[8] Liu, C. M., Lin, H. W., Huang, Y. S., Chu, Y. C., Chen, C., Lyu, D. R., ... & Tu, K. N., 'Low-temperature direct copper-to-copper bonding enabled by creep on (111) surfaces of nanotwinned Cu', *Sci Rep*, vol. 5, no. 1, p. 9734, 2015.
[9] A. Kotri, E. El Koraychy, M. Mazroui, and I. Achik, 'Hetero-diffusion of small clusters on Ag (111) surface', *The European Physical Journal Plus*, vol. 133, pp. 1–8, 2018.
[10] A. Kotri, Y. Belkassmi, E. Elkoraychy, M. Mazroui, and L. Elmaimouni, 'Static investigation of the small clusters on the Cu (111) and Au (111) surfaces', *Chinese Journal of Physics*, vol. 73, pp. 552–560, 2021.
[11] T.-H. Chuang, P.-C. Wu, Y.-C. Lai, and P.-I. Lee, 'Low-Temperature Direct Bonding of 3D-IC Packages and Power IC Modules Using Ag Nanotwinned Thin Films', *International Journal of Manufacturing, Materials, and Mechanical Engineering (IJMMME)*, vol. 12, no. 1, pp. 1–16, 2022.
[12] P.-C. Wu, Y.-C. Lai, and T.-H. Chuang, 'Enhancing effect of substrate bias on nanotwin formation of sputtered Ag thin films', *Journal of Materials Science: Materials in Electronics*, vol. 32, no. 17, pp. 21966–21973, 2021.
[13] H. H. T. and C. H. C. T.H. Chuang, 'Die bonding structure and method of manufacturing the same ', 2024
[14] T. Hsing-Hua, A. Chuang, P.-C. Wu, and C. Chung-Hsin, 'Silver nano-twinned thin film structure and method for forming the same'. Google Patents, Nov. 01, 2022.
[15] P.-C. Wu, Y.-C. Lai, and T.-H. Chuang, 'Enhancing effect of substrate bias on nanotwin formation of sputtered Ag thin films', *Journal of Materials Science: Materials in Electronics*, vol. 32, no. 17, pp. 21966–21973, 2021.
[16] Z.-H. Yang, P.-C. Wu, and T.-H. Chuang, 'Effects of substrate bias on the sputtering of high density (111)-nanotwinned Cu films on SiC chips', *Sci Rep*, vol. 12, no. 1, p. 15408, 2022.
[17] D. I. Syafei, M.-T. Chiang, and T.-H. Chuang, 'Formation of Cu Nanotwins on Silicon Carbide Wafers with Cr Adhesive Layer under Various Substrate Bias', *Metals (Basel)*, vol. 13, no. 10, p. 1747, 2023.
[18] P. M. Agrawal, B. M. Rice, and D. L. Thompson, 'Predicting trends in rate parameters for self-diffusion on FCC metal surfaces', *Surf Sci*, vol. 515, no. 1, pp. 21–35, 2002.
[19] Liu, C. M., Lin, H. W., Huang, Y. S., Chu, Y. C., Chen, C., Lyu, D. R., ... & Tu, K. N.., 'Low-temperature direct copper-to-copper bonding enabled by creep on (111) surfaces of nanotwinned Cu', *Sci Rep*, vol. 5, no. 1, p. 9734, 2015.
[20] M. Myśliwiec and R. Kisiel, 'Applying sintering and SLID bonding for assembly of GaN chips working at high temperatures', in *2018 7th Electronic System-Integration Technology Conference (ESTC)*, IEEE, 2018, pp. 1–5.
[21] H.-Q. Zhang, H.-L. Bai, Q. Jia, W. Guo, L. Liu, and G.-S. Zou, 'High electrical and thermal conductivity of nano-Ag paste for power electronic applications', *Acta Metallurgica Sinica (English Letters)*, vol. 33, pp. 1543–1555, 2020.
[22] T. Watanabe, M. Takesue, T. Matsuda, T. Sano, and A. Hirose, 'Thermal stability and characteristic properties of pressureless sintered Ag layers formed with Ag nanoparticles for power device applications', *Journal of Materials Science: Materials in Electronics*, vol. 31, pp. 17173–17182, 2020.
[23] P.-C. Wu, Y.-C. Lai, P.-I. Lee, M.-T. Chiang, J. Chou, and T.-H. Chuang, 'Sputtering of Ag (111) nanotwinned films on Si (100) wafers for backside metallization of power devices', *Journal of Materials Science: Materials in Electronics*, vol. 32, pp. 7319–7329, 2021.
[24] Y. Liu, H. Zhang, L. Wang, X. Fan, G. Zhang, and F. Sun, 'Effect of sintering pressure on the porosity and the shear strength of the pressure-assisted silver sintering bonding', *IEEE Transactions on Device and Materials Reliability*, vol. 18, no. 2, pp. 240–246, 2018.
[25] L.-P. Chang, J.-J. Wang, and F.-Y. Ouyang, 'Improvement of Ag films with highly (111) surface orientation for metal direct bonding technique: Nanotwinned structure and ion bombardment effect', *Mater Chem Phys*, vol. 274, p. 125159, 2021.
[26] T.-H. Chuang, Y.-T. Chen, Y.-H. Chen, C.-C. Chu, and C.-S. Lin, 'Improvement of Silver Sintered Die Bonding of SiC/DBC Power Modules through Backside Metallization with High Density (111) Orientation Ag Nanotwinned Films', *IEEE Trans Compon Packaging Manuf Technol*, 2024.
[27] Weng, W. L., Chen, H. Y., Ting, Y. H., Chen, H. Y. T., Wu, W. W., Tu, K. N., & Liao, C. N., 'Twin-Boundary Reduced Surface Diffusion on Electrically Stressed Copper Nanowires', *Nano Lett*, vol. 22, no. 22, pp. 9071–9076, 2022.